Chapter 6. Ni(II), Ni(I), and Ni(0) complexes supported by the isopropyl-substituted tris(phosphino)borate, $[PhB(CH_2P^iPr_2)_3]^-$

MacBeth, C. E.; Thomas, J. C.; Betley, T. A.; Peters, J. C. *Inorg. Chem.* **2004**, *43*, *in press*.

6.1. Introduction

The fundamental coordination chemistry of mid-to-late first row transition metal ions supported by relatively simple ligand auxiliaries represents a mature field that has been revived in recent years. Much of this recent interest arises from the possibility of these species to participate in catalytic group transfer reactions such as aziridinations,[1] cyclopropanations,[2] and oxidations.[3] Additionally, new approaches to catalytic small molecule activation and functionalization reactions that exploit reactive metal fragments from this sector of the transition block may yet be elucidated, including substrates such as organic azides, N_2O, O_2, CO_2, and CO.[4-6] One attractive feature of the mid-to-late first row ions is their potential to form metal-to-ligand multiple bonds that are kinetically and thermodynamically reactive. Species such as a metal-oxo, -carbene, -imide, or -nitride have been proposed as key intermediates in catalytic reactions of both synthetic and biocatalytic significance.[3,7]

Very recently, several groups have reported the isolation of well-defined nickel complexes containing metal-to-ligand multiple bonds. For example, using sterically encumbering bis(phosphine) ligands, Hillhouse and coworkers have shown that L_2Ni fragments are compatible with imide (NR),[8] phosphinidene (PR),[9] and carbene (CR_2)[10] functional groups (described here as L_2Ni^{II}=E species). These complexes, which build on an early observation from Jones' group that provided strong evidence for a reactive L_2Ni^{II}=S fragment,[11] have since been shown to undergo stoichiometric group transfer processes.[12,13] These three-coordinate L_2Ni^{II}=E systems owe their stability to a combination of electronic factors and the considerable steric protection provided by both the bulky bis(phosphine) ligand and the bulky substituents at the multiply bonded functional group. Similarly, the Warren group has demonstrated more recently that

Ni^{III}=E multiple bonds are accessible using three-coordinate L_2Ni=E platforms where the L_2 scaffold is a sterically encumbered anionic betadiketiminate.[14]

Four-coordinate pseudo-tetrahedral systems that feature M=E and M≡E bonds on mid-to-late first row metals (described here as L_3M≡E systems) are equally intriguing target molecules. Recent findings from our laboratory have shown that 'L_3Co' and 'L_3Fe' complexes supported by the anionic tris(phosphine) donors [$PhBP_3$] or [$PhBP^{iPr}_3$] ([$PhBP_3$] = [$PhB(CH_2PPh_2)_3]^-$, [$PhBP^{iPr}_3$] = [$PhB(CH_2P^iPr_2)_3]^-$) (i) will support metal-to-ligand triple bonds (e.g., [$PhBP_3$]Co≡N(*p*-tolyl)) and (ii) will participate in two-electron group transfer reactions that accept and release the multiply bonded functional unit.[15-17] In addition, Theopold's group has recently demonstrated that a sterically encumbered tris(pyrazolyl)borate ligand can support similar metal-to-ligand multiple bonds on cobalt.[18] In a related tripodal system, Riordan's group has shown that '$L_3Ni(I)$' species containing anionic tris(thioether)borate ligands can undergo oxidative group transfer. For example, a Ni(I) carbonyl has been shown to react with dioxygen to form an Ni_2O_2 diamond core motif in which each nickel center is formally trivalent.[19] This structure type was first elucidated by Hikichi and coworkers using a tris(pyrazolyl)borate auxiliary scaffold.[20]

An understanding of the electronic structures that might give rise to isolable later first row metal M=E and M≡E multiple bonds for three- or four-coordinate complexes remains to be developed. This type of information is essential if we are to understand the fundamental reactivity patterns of such species. Motivated by the results of the Hillhouse and Theopold groups as well as our own findings, our group recently initiated the development of 'L_3NiX' platforms using the tris(phosphino)borate ligands [$PhBP_3$] and

[$PhBP^{iPr}_3$]. In this chapter, di-, mono- and zerovalent nickel complexes supported by the [$PhBP^{iPr}_3$] scaffold are described. We focus on fundamental aspects of the synthesis and characterization of these complexes, and we discuss reactivity issues pertinent to the possible construction of $L_3Ni{=}E$ and $L_3Ni{\equiv}E$ bonds. Where applicable, structural and electronic comparisons are made between the related '[$PhBP^{iPr}_3$]Ni' and '[$PhBP_3$]Ni' systems as well as their structurally similar counterparts supported by other anionic or neutral facially capping ligand auxiliaries.[21-24] At this stage, it is clear that tris(phosphino)borate scaffolds effectively support the lower oxidation states of nickel (e.g., Ni^0, Ni^I, and Ni^{II}) while in most cases maintaining a four-coordinate pseudo-tetrahedral geometry. Synthetic access to $L_3Ni^{III}{\equiv}E$ and $L_3Ni^{IV}{\equiv}E$ species remains problematic, however. Based upon molecular orbital arguments supported by DFT calculations, we suspect that the difficulty in accessing these species is synthetic in nature. We believe that higher oxidation states supported by nickel-to-ligand multiple bonds should be stable, but conditions for their clean generation remain to be elucidated.

6.2. Results and discussion

6.2.1. Synthesis and characterization of pseudo-tetrahedral [$PhBP_3$]NiX and [$PhBP^{iPr}_3$]NiX complexes

A synthetic precursor to the nickel chemistry described here is the Ni(II) halide [$PhBP^{iPr}_3$]NiCl (**6.1**). Analogous divalent complexes have been reported previously for [$PhBP_3$]- and [$PhBP^{iPr}_3$]-supported iron and cobalt systems,[25] and a synthetic protocol using [$PhBP^{iPr}_3$]Tl as a transmetalation reagent is equally effective for nickel. Thus, the synthesis of the yellow-green S = 1 complex [$PhBP^{iPr}_3$]NiCl (**6.1**) is achieved in high isolated yield (>90%) by reacting (DME)$NiCl_2$ (DME = 1,2-dimethoxyethane) with [$PhBP^{iPr}_3$]Tl. An Evans' method measurement of **6.1** in benzene solution is consistent

with two unpaired electrons per nickel center (μ_{eff} = 2.97 μ_B). The reaction of [PhBP$^{iPr}_3$]Tl with other Ni(II) precursors, such as $(Ph_3P)_2NiCl_2$ and $NiCl_2$, provides some quantity of **6.1**; however, the desired product is accompanied by large amounts of diamagnetic impurities in each case. In contrast, [PhBP$_3$]Tl reacts with the nickel precursors $(Ph_3P)_2NiCl_2$ or NiI_2 to generate green [PhBP$_3$]NiCl and red-brown [PhBP$_3$]NiI halide complexes respectively. We suggest that the undesirable side-products that can arise during attempts to install the [PhBP$^{iPr}_3$] ligand on nickel are due to competitive redox reactions in which the borate anion reduces the Ni(II) center. These types of electron-transfer reactions would generate a reactive borane radical that then may undergo bond homolysis to liberate a $\cdot CH_2PR_2$ radical. The [PhBP$^{iPr}_3$] anion is inherently more reducing than its [PhBP$_3$] counterpart, and, as a result, its installation at nickel is somewhat more sensitive.

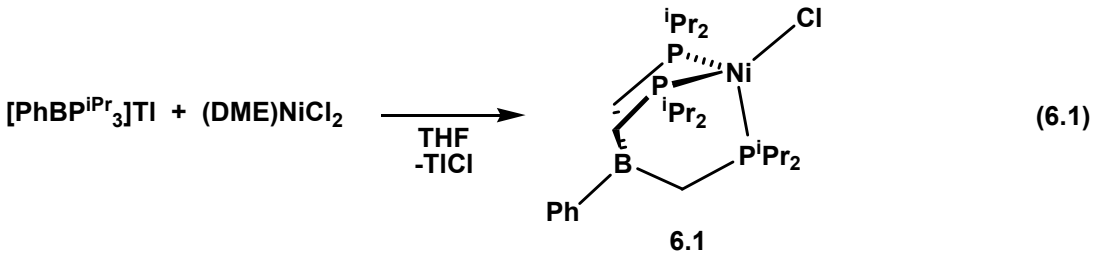

The solid-state structure of **6.1** was determined by X-ray diffraction studies on a single crystal of **6.1** (Figure 6.1). The halide complex is four-coordinate and pseudo-tetrahedral, and the bond lengths and angles are unremarkable. Although a limited number of pseudo-tetrahedral tris(phosphine) nickel(II) iodide and bromide complexes have been structurally characterized, no examples of pseudo-tetrahedral tris(phosphine) nickel(II) chlorides have been reported. The structure of **6.1** compares well with the structurally related [PhBP$_3$]NiI. Both tris(phosphine) halide complexes contain Ni-P

bond lengths between 2.26 and 2.29 Å. The P-Ni-P angles are on average slightly larger for **6.1** (94-95º) than for [PhBP$_3$]NiI (91.5-94º). In general, the structural parameters for **6.1** show a more threefold symmetric environment than that found in [PhBP$_3$]NiI.

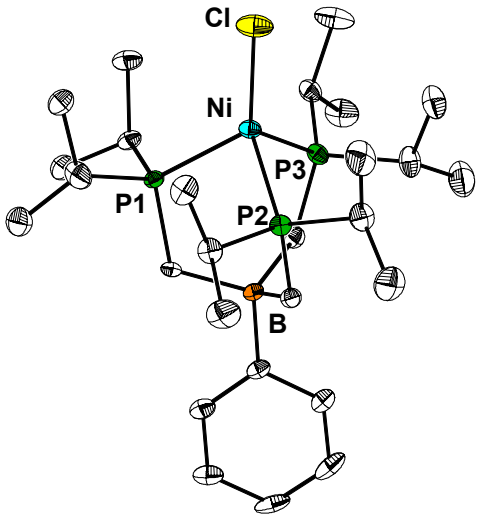

Figure 6.1. Displacement ellipsoid representation (50%) of [PhBP$^{iPr}_3$]NiCl (**6.1**). Hydrogen atoms have been omitted for clarity. Selected interatomic distances (Å) and angles (º) for **6.1**: Ni-Cl, 2.1772(9); Ni-P1, 2.2871(8); Ni-P2, 2.2893(9); Ni-P3, 2.2811(8); Ni-B, 3.474(3); P1-Ni-P2, 94.12(3); P2-Ni-P3, 94.97(3); P1-Ni-P3, 94.16(3); Cl-Ni-P1, 125.30(4); Cl-Ni-P2, 121.92(4); Cl-Ni-P3, 118.94(3).

6.2.2. Electrochemical data for divalent complexes

The tris(phosphino)borate ligands [PhBP$_3$] and [PhBP$^{iPr}_3$] stabilize monovalent forms of both iron and cobalt. These complexes have proven effective for the installation of metal-ligand multiple bonds via oxidative group transfer.[15-17] To determine the accessibility of the Ni(I) state in these tris(phosphino)borate nickel systems, we first studied the cyclic voltammetry of the divalent halide precursors. These studies were performed in THF using [^{n}Bu$_4$N][PF$_6$] (0.35 M) as the supporting electrolyte. All data are referenced to Fc/Fc$^+$ (Fc = ferrocene, Fc$^+$ = ferrocenium) as an internal standard using

$Ag/AgNO_3$ as the reference electrode. Figure 6.2 comparatively shows the first reduction process observed for the halide complexes $[PhBP_3]NiCl$, $[PhBP_3]NiI$, and **6.1**. We assign each process as a one-electron reduction of $L_3Ni^{II}X$ to $[L_3Ni^{I}X]^-$. The reduction event for the chloride complex $[PhBP_3]NiCl$ is fully reversible at -1.20 V (Figure 6.2b). The $Ni^{II/I}$ couple shifts to -1.12 V (Figure 6.2c) on replacement of chloride by the weaker field iodide ligand in $[PhBP_3]NiI$. The first reduction event observed for **6.1** is at appreciably lower potential (-1.44 V, Figure 6.2a) and is only quasireversible at 100 mV/s. Increasing the concentration ($\geq 1x10^{-3}$ M) of **6.1** results in rapid deposition of material on the glassy carbon electrode and disappearance of the reduction wave. The $Ni^{II/I}$ couple for **6.1** as compared to $[PhBP_3]NiCl$ ($\Delta E_{1/2}$ = 240 mV) reflects the large difference in electron-releasing character of the $[PhBP^{iPr}_3]$ ligand relative to its $[PhBP_3]$ counterpart. We have noted this distinction previously from analysis of the cyclic voltammograms of the complexes $[PhBP^{iPr}_3]FeCl$ and $[PhBP_3]FeCl$ ($\Delta E_{1/2}$ = 322 mV).[16,25b] The cyclic voltammetry of complexes $[PhBP_3]NiCl$, $[PhBP_3]NiI$, and **6.1** failed to show an oxidation wave within the detectable range under the conditions used (below 1.0 V). In comparison to previously described $L_3Ni^{II}X$ systems, the cationic tripodal phosphine system $[\{CH_3C(CH_2PPh_2)_3\}NiX][ClO_4]$, where X = Cl or I, showed reversible $Ni^{II/I}$ couples at -0.53 V and -0.43 V (vs. Fc/Fc^+) for the chloride and iodide, respectively, in CH_2Cl_2 solution.[26,27] The $Ni^{II/I}$ couples for these cationic complexes are significantly more positive as compared to the neutral complexes $[PhBP_3]NiCl$, $[PhBP_3]NiI$, and **6.1**. This correlates with our understanding that the monoanionic tris(phosphino)borate ligands result in a more electron-rich metal center relative to structurally similar neutral trisphosphine ligands. To provide a comparison with a related neutral pseudo-tetrahedral

nickel(II) system, Riordan has reported a $Ni^{II/I}$ irreversible reduction potential at -1.3 V (versus Fc/Fc^+ in CH_2Cl_2) for the tris(thioether)borate complex $[PhTt^{tBu}]NiCl$ ($[PhTt^{tBu}] = [PhB(CH_2S^tBu)_3]^-$).[28] This reduction potential resides within the range of $Ni^{II/I}$ reduction potentials observed for $[PhBP_3]NiCl$, $[PhBP_3]NiI$, and **6.1**, but unlike the tripodal phosphine-ligated systems, is not reversible.

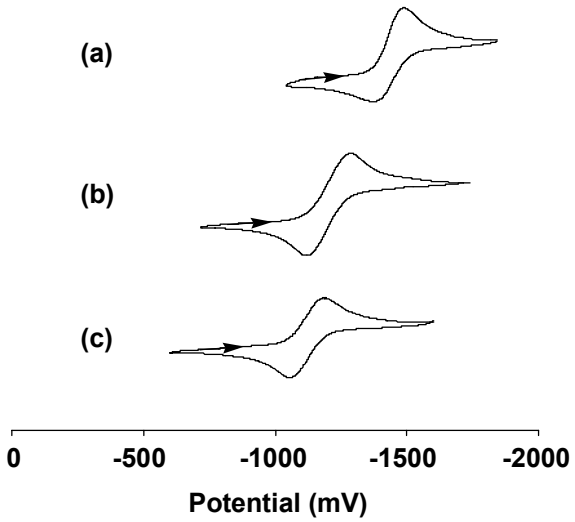

Figure 6.2. Cyclic voltammograms of (a) **6.1**, (b) $[PhBP_3]NiCl$, and (c) $[PhBP_3]NiI$ recorded at a scan rate of 100 mV/s. Potentials are referenced to Fc/Fc^+.

6.2.3. Chemical reduction and metathesis of $[PhBP^{iPr}_3]NiCl$

Given the electrochemical stability of monovalent nickel within these P_3NiX platforms, it was of interest to prepare Ni(I) complexes for subsequent group transfer studies. The chemistry of Ni(I) complexes has only recently been undertaken in a systematic fashion. Hillhouse's group has prepared P_2Ni^IX complexes that feature halides, pseudo-halides, and alkyls as the X-ligand.[8-10] Also, Riordan's group has made use of tris(thioether)borate ligands such as $[PhTt^{tBu}]$ to stabilize Ni(I). For example, reduction of $[PhTt^{tBu}]NiCl$ by methyl lithium under an atmosphere of CO provides

[PhTt^{tBu}]Ni(CO).[29] Other Ni(I) complexes supported by betadiketiminate ligands have also been described recently.[14,30]

The reduction of [PhBP$^{iPr}_3$]NiCl (**6.1**) was attempted with several typical reductants such as sodium amalgam, sodium naphthelenide, KC_8, Mg, and (9,10-dihydro-9,10-anthracenediyl)tris(tetrahydrofuran)magnesium. The reaction mixtures generated upon reduction of **6.1** in the absence of a suitable additional donor ligand showed primarily diamagnetic products by both ^{1}H and ^{31}P{^{1}H} NMR spectroscopy, and the mixtures are ill-defined. In several cases, the formation of ^{i}Pr$_2$PMe was evident in the ^{31}P{^{1}H} NMR spectra, suggesting some degree of [PhBP$^{iPr}_3$] degradation. In most of the reduction reactions, resonances consistent with diamagnetic Ni-H species, where the hydride signal is coupled to phosphorus nuclei, were apparent in the ^{1}H NMR spectra (-10 to -15 ppm). Unlike the reduction of the related [PhBP$_3$]NiCl, the ligand decomposition product [PhBP$^{iPr}_3$]Ni(η^2-CH$_2$P^{i}Pr$_2$) (**6.2**) was not formed as determined by ^{1}H and ^{31}P{^{1}H} NMR spectroscopy.

Diamagnetic yellow **6.2** was prepared independently by reaction of **6.1** with ^{i}Pr$_2$PCH$_2$Li in THF (eq 6.2). The five-coordinate nature of **6.2** was evident in its ^{1}H, ^{31}P{^{1}H}, and ^{13}C{^{1}H} NMR spectra. For example, the ^{13}C{^{1}H} NMR spectrum contained a resonance at -12.84 ppm with a doublet of quartets pattern. Similarly, the ^{31}P{^{1}H} NMR spectrum showed two resonances: a quartet at 1.2 ppm and a broad peak centered at 49 ppm. These data indicate that the phosphines of the tris(phosphino)borate ligand are magnetically exchanging rapidly in solution while remaining bound to nickel. The coupling patterns seen for the "^{i}Pr$_2$PCH$_2$" fragment also indicate that both the

methylene and the phosphine are bound to nickel. Thus, we believe that diamagnetic **6.2** is five-coordinate in solution.

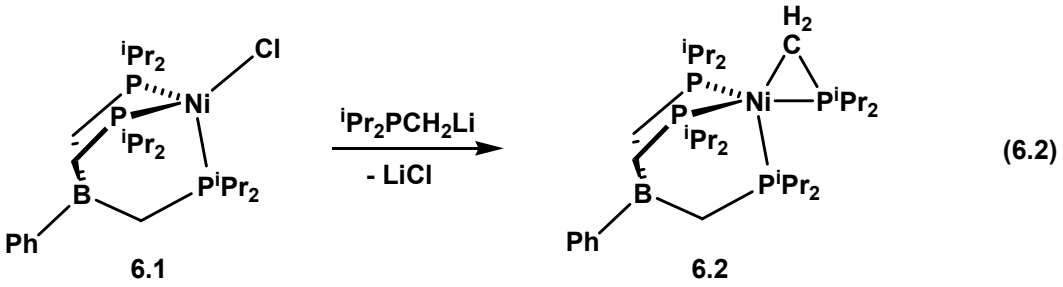

(6.2)

As observed in our electrochemical studies, the [$PhBP^{iPr}_3$] anion lowers the reduction potential of the divalent nickel state considerably. We therefore thought that [$PhBP^{iPr}_3$]NiCl might provide clean substitution chemistry with potentially reducing nucleophiles rather than problematic electron transfer chemistry. The reactivity of **6.1** was therefore explored with lithiated amines. One example of note is the lithium amide Li(dbabh) (Hdbabh = 2,3:5,6-dibenzo-7-azabicyclo[2.2.1]hepta-2,5-diene),[31] chosen as a possible N-atom transfer reagent (*vide infra*). The reaction between **6.1** and Li(dbabh) at low temperature results in an opaque green-brown solution from which the three-coordinate nickel(II) complex [κ^2-$PhBP^{iPr}_3$]Ni(dbabh) (**6.3**) can be isolated (eq 6.3). The three coordinate nature of **6.3** in solution is strongly suggested by its NMR data, which show a diamagnetic product. Only one phosphine environment is evident by both ^{1}H NMR and ^{31}P{^{1}H} NMR spectroscopy, indicating that the phosphine ligands of **6.3** are in rapid exchange on the NMR time scale.

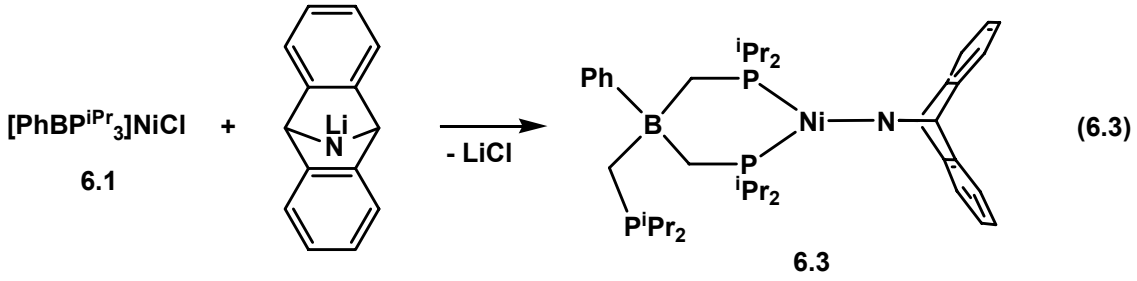

(6.3)

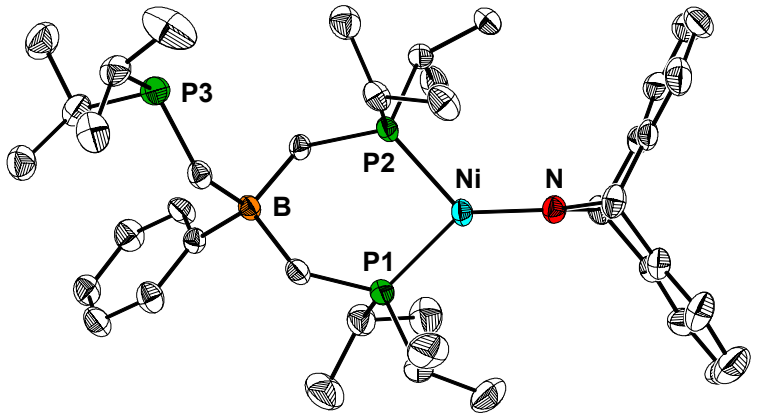

Figure 6.3. Displacement ellipsoid representation (50%) of [κ^2-PhBP$^{iPr}_3$]Ni(dbabh) (**6.3**). Hydrogen atoms have been omitted for clarity. Selected distances (Å) and angles (º): P1-Ni, 2.1475(7); P2-Ni, 2.1317(7); N-Ni, 1.748(2); P1-Ni-P2, 93.38(3); P1-Ni-N, 136.86(7); P2-Ni-N, 129.65(7).

Definitive assignment of the structure of **6.3** is provided by its solid-state molecular structure (Figure 6.3). As can be seen, the amide ligand adopts a conformation such that its available π-orbital lies in the P_2Ni plane. This conformation is similar to related (dtbpe)Ni^I-NR_2 species prepared by the Hillhouse group (dtbpe = $^tBu_2PCH_2CH_2P^tBu_2$). When comparing **6.3** to other nickel-amide complexes, it is interesting to note that their Ni-N distance ranges from 1.82 to 1.93 Å, approximately 0.1 Å longer than that observed for **6.3** (1.748(2) Å). The Ni-N distance of **6.3** (1.748(2) Å) is quite similar, however, to that reported for [(dtbpe)Ni-NH{2,6-$(CHMe_2)_2C_6H_3$}] [PF_6] (1.768(14) Å). The short Ni-N bond length suggests a significant π-interaction, consistent with the orientation of the amide ligand. The dechelation of one phosphine ligand in **6.3** is likely favored due to this π-interaction. In addition to Li(dbabh), the reaction between **6.1** and the lithium anilides Li(NHPh) and Li{NH(2,6-diisopropylphenyl)} also suggests the formation of three coordinate Ni^{II}-NR_2 structures. These products are likewise diamagnetic and give highly colored solutions

(red and purple, respectively). Our evidence shows that the $[PhBP^{iPr}_3]Ni^{II}$ scaffold is more resistant to outer-sphere reduction than the related $[PhBP_3]Ni^{II}$ system and allows for cleaner substitution to occur at the Ni(II) state. However, the pseudo-tetrahedral geometry is compromised by dechelation of one phosphine donor.

6.2.4. Synthesis and characterization of $[PhBP^{iPr}_3]Ni^{I}L$ complexes

The presence of a suitable L-type trapping ligand can stabilize the Ni(I) state during reduction of $[PhBP^{iPr}_3]NiCl$ (**6.1**) to give synthetically useful $P_3Ni^{I}L$ complexes (eq 6.4). Reducing **6.1** using a sodium amalgam in the presence of excess PMe_3 (5 equivalents) results in analytically pure bright yellow $[PhBP^{iPr}_3]Ni(PMe_3)$ (**6.4**) after isolation. Yellow **6.4** also forms by reacting the Ni(0) precursor $Ni(PMe_3)_4$ with $[PhBP^{iPr}_3]Tl$. This latter reaction proceeds with concomitant reduction of Tl(I) to Tl(0), evident by the precipitation of thallium metal from solution. Crystals of **6.4** were obtained from this reaction by crystallization from diethyl ether at -30 °C. X-ray crystallographic analysis showed that the crystals contained a 95:5 mixture of **6.4** and $[PhBP^{iPr}_3]Tl$. The presence of a small amount of $[PhBP^{iPr}_3]Tl$ in the crystals was also visible from their $^{31}P\{^{1}H\}$ NMR spectrum and by the presence of a well-refined peak in the difference Fourier map attributable to the presence of thallium. The molecular structure of **6.4** (Figure 6.4A) shows a four-coordinate and pseudo-tetrahedral Ni(I) center very similar to that observed for the related complex $[PhBP_3]Ni(PPh_3)$. Measurement of the magnetic moment of analytically pure **6.4** by Evans' method in benzene solution provides $\mu_{eff} = 1.82\ \mu_B$, consistent with one unpaired electron for the d^9 electronic configuration.

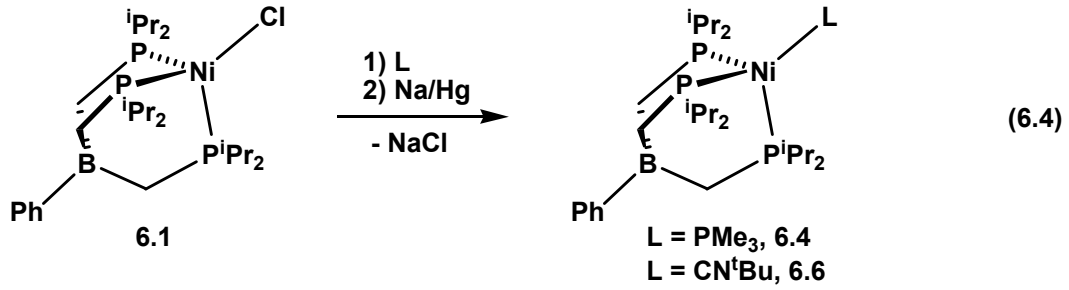

(6.4)

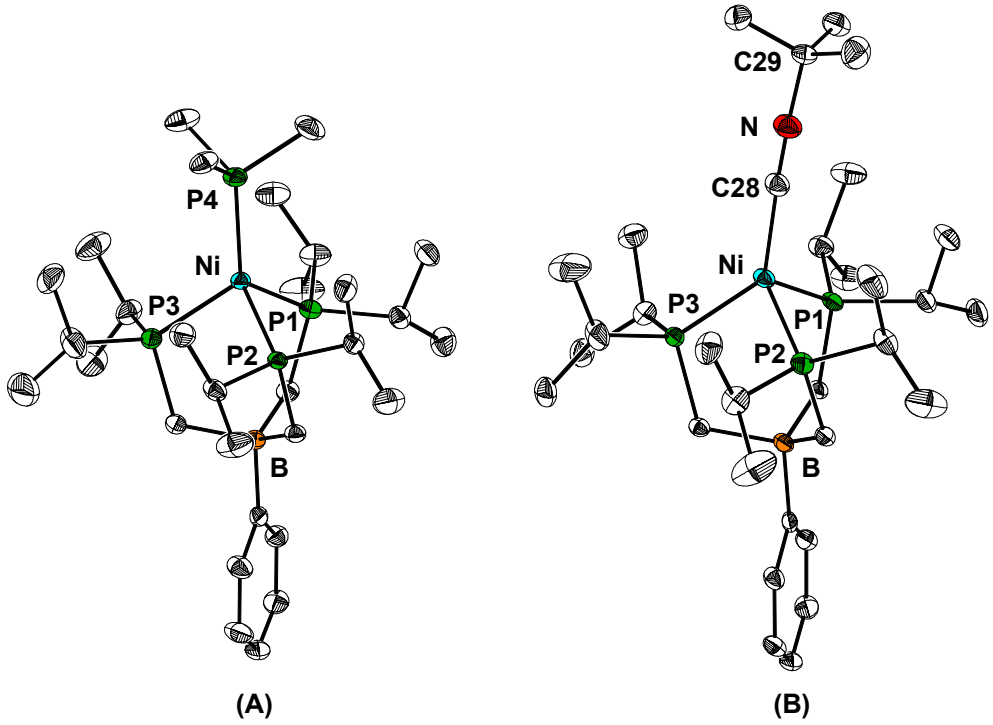

Figure 6.4. Displacement ellipsoid representations (50%) of (A) [PhBP$^{iPr}_3$]Ni(PMe$_3$) (**6.4**), and (B) [PhBP$^{iPr}_3$]Ni(CN^{t}Bu) (**6.6**). Hydrogen atoms omitted for clarity. Selected interatomic distances (Å) and angles (º) for **6.4**: Ni-P1, 2.2533(5); Ni-P2, 2.2764(5); Ni-P3, 2.2873(5); Ni-P4, 2.2631(5); Ni-B, 3.436(2); P1-Ni-P4, 118.67(2); P2-Ni-P4, 121.90(2); P3-Ni-P4, 123.43(2); P1-Ni-P2, 92.76(2); P2-Ni-P3, 98.24(2); P3-Ni-P1, 94.74(2). For **6.6**: Ni-C28, 1.864(2); Ni-P1, 2.2403(5); Ni-P2, 2.2749(6); Ni-P3, 2.2562(6); Ni-B, 3.431(2); P1-Ni-P2, 96.83(2); P1-Ni-P3, 93.50(2); P2-Ni-P3, 96.42(2); P1-Ni-C28, 104.56(6); P2-Ni-C28, 124.37(7); P3-Ni-C28, 131.79(7).

A [PhBP$^{iPr}_3$]-ligated Ni(I) isocyanide complex has also been prepared by a similar method. Addition of excess ^{t}BuNC (approximately 5 equivalents) to **6.1** in THF solution

results in the initial formation of a red, likely square planar Ni(II) complex, [κ^2-PhBP$^{iPr}_3$]Ni(Cl)(CN^{t}Bu) (**6.5**). Assignment of the square planar species is based upon its $^{31}P\{^1H\}$ NMR spectrum (δ 62.7 (br d), 47.7 (br d), 3.2 (br s)). Removal of the reaction volatiles followed by redissolution in THF and subsequent reduction using sodium amalgam provides the yellow Ni(I) complex [PhBP$^{iPr}_3$]Ni(CN^{t}Bu) (**6.6**). Attempts to reduce **6.1** in the presence of excess ^{t}BuNC result in the formation of an increased number of side products, presumably due to the competitive reduction of isocyanide. Complex **6.6** is more readily prepared in high yield by the reaction of **6.4** with excess CN^{t}Bu (approximately 5 equivalents), which substitutes PMe_3. The solution magnetic moment of **6.6** as determined by Evans' method is consistent with the d^9 configuration (μ_{eff} = 1.68 μ_B). Examination of the IR spectrum of **6.6** provides a ν_{CN} stretching frequency of 2056 cm^{-1} (KBr, THF). The increased electron-releasing character of [PhBP$^{iPr}_3$] versus [PhBP$_3$] is evident from the ν_{CN} vibrations recorded for **6.6** and the related complex [PhBP$_3$]Ni(CN^{t}Bu) (ν_{CN} = 2094 cm^{-1}), the former being shifted to lower energy by 38 cm^{-1}. The solid-state structure of **6.6** (Figure 6.4B), however, is very similar to that found for [PhBP$_3$]Ni(CN^{t}Bu).[32] Hence, the comparison of isocyanide stretching frequencies is a good qualitative electronic assessment of the [PhBP$^{iPr}_3$] and [PhBP$_3$] anions. To the best of our knowledge, complexes **6.6** and [PhBP$_3$]Ni(CN^{t}Bu) are the only structurally characterized, mononuclear Ni(I) isocyanide complexes.

6.2.5. Access to the Ni(0) state

Having prepared Ni(I) complexes, we examined their electrochemical potentials. The cyclic voltammetries of the Ni(I) complexes **6.4** and **6.6** were studied in THF solution. As shown in Figure 6.5b, the phosphine adduct **6.4** displays a reversible event

at -1945 mV, assigned as a $Ni^{I/0}$ couple. An irreversible oxidation also occurs at -503 mV. Similarly, **6.6** shows a reversible low reduction potential event assigned as a $Ni^{I/0}$ couple (-1848 mV) (Figure 6.5a), and an irreversible oxidation event (-396 mV). The shift to more positive potentials for both processes for **6.6** as compared to **6.4** reflects the exchange of an electron-donating phosphine ligand for a π-acidic isocyanide ligand. Both complexes show the presumed Ni(0) reduction processes at quite low potentials.

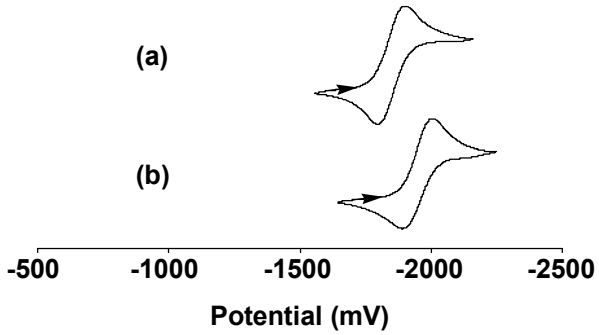

Figure 6.5. Cyclic voltammograms of (a) **6.6** and (b) **6.4** recorded at a scan rate of 50 mV/s. Potentials are referenced to Fc/Fc^{+}.

Based on these electrochemical observations, we studied the independent chemical reduction of **6.4**. As suggested from the formation of **6.4** by the reaction between $[PhBP^{iPr}_3]Tl$ and $Ni(PMe_3)_4$, the putative Ni(0) anion $\{[PhBP^{iPr}_3]Ni(PMe_3)\}^-$ (**6.7**) is generated at very low potential. Anionic $\{[PhBP^{iPr}_3]Ni(PMe_3)\}^-$ appears to be accessible by reduction of **6.4** with strong alkali metal reductants, such as sodium amalgam or KC_8, in THF solution. Examination of the ^1H NMR spectra of such reduction reactions shows complete consumption of paramagnetic **6.4** and the presence of broadened diamagnetic resonances consistent with a fluxional Ni(0) anion. In THF solution, these complexes have limited stability and ultimately re-oxidize to Ni(I) **6.4** by mechanisms that we do not currently understand. The reduction chemistry of neutral **6.6**

was also studied. Similarly, chemical reduction of **6.6** using strong reductants such as KC_8 or sodium amalgam results in its complete consumption and the formation of a diamagnetic species (^{1}H NMR). The solution infrared spectrum of this product shows a dramatically shifted ν_{CN} vibration (1982 cm^{-1}, compared with 2056 cm^{-1} for **6.6**), indicating the presence of the Ni(0) anion $\{[PhBP^{iPr}_3]Ni(CN^tBu)\}^-$ (**6.8**). This species is also unstable in benzene or THF solution and gradually decays to regenerate the Ni(I) species **6.6** as the predominant product. Whether some type of disproportionation reaction or reaction with solvent occurs is presently unclear. The degradation process to reform **6.6** is quite clean, suggesting the involvement of some external electron-acceptor.

Access to isolable Ni(0) was achieved by reaction of the tris(phosphino)borate ligand with $(Ph_3P)_2Ni(CO)_2$. Reacting $[PhBP^{iPr}_3]Tl$ with $(Ph_3P)_2Ni(CO)_2$ in the presence of ASNBr (ASN = 5-azoniaspiro[4.4]nonane) in THF solution proceeds over four days at room temperature to form $[[\kappa^2\text{-}PhBP^{iPr}_3]Ni(CO)_2][ASN]$ (**6.9**) (eq 6.5). The substitution reaction is significantly slower for $[PhBP^{iPr}_3]$ than for $[PhBP_3]$ (12 h). Attempts to accelerate the reaction via mild heating (50 °C) resulted in extensive decomposition of the starting material to unidentified products. Complex **6.9** displays characteristic signals in its infrared spectrum (ν_{CO} = 2004 and 1878 cm^{-1}; KBr, THF) and $^{31}P\{^1H\}$ NMR spectrum (δ 51.1 (s, 2P), 4.8 (s, 1P), corresponding to its coordinated and dissociated phosphines, respectively). The ν_{CO}(avg) for **6.9** (1941 cm^{-1}) is consistent with the more electron-donating isopropyl groups relative to the phenyl substituents of $[[\kappa^2\text{-}PhBP_3]Ni(CO)_2][TBA]$ (ν_{CO}: 1994, 1913 cm^{-1}, ν_{CO}(avg): 1951 cm^{-1}; KBr, THF). Attempts to oxidize **6.9** using $[Fc][PF_6]$ to give well-defined Ni(I) monocarbonyl products instead led to multiple products as determined by IR and NMR spectroscopy.

Given the stability of Riordan's [PhTt^{tBu}]Ni^{I}(CO) and related Ni(I) carbonyls, we suspect over-oxidation to be problematic in the present reactions and that gentler oxidants may prove effective.

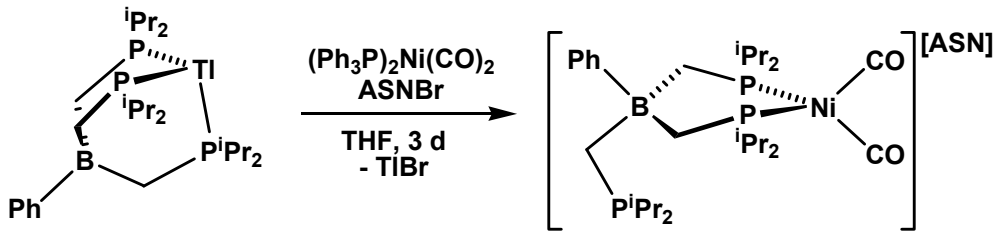

(6.5)

6.9

6.2.6. Synthetic attempts to generate Ni=E/Ni≡E bonds

One goal of this study was to assess the propensity of the low valent nickel precursors described herein to mediate oxidative group transfer processes to install Ni=E/Ni≡E multiple bonds at the pseudo-tetrahedral nickel site. We have attempted many reactions that might have led to such species. To date, we have not been able to isolate well-defined examples of such species. Several of these attempts are summarized here.

One target we attempted to prepare was a tetravalent nickel state stabilized by a terminal nitride functionality. We suspected that such a species might be unstable, but the hypothetical d^6 L$_3$Ni^{IV}≡N fragment would be isolobal and isoelectronic to d^6 L$_3$Co^{III}≡NR species we have prepared previously.[15,17] Based upon molecular orbital considerations, there is no reason to assume that such a structure type should be synthetically inaccessible, although subsequent reaction pathways may dominate under reaction conditions. One route to the terminal nitride is a two-electron oxidative N-atom transfer from the dbabh amide to Ni(II) with concomitant loss of anthracene. Precedence for this type of transformation has been provided by Mindiola and Cummins in the

synthesis of a $Cr^{VI}\equiv N$ nitride and more recently by Betley and Peters in the formation of $[PhBP^{iPr}_3]Fe(N)$.[31,33] As described above, the reaction between Li(dbabh) and **6.1** did generate a Ni^{II}-N amide, but the stable product is the trigonal planar three-coordinate Ni^{II} species **6.3**. We had hoped that the electron-rich nature of the $[PhBP^{iPr}_3]$ ligand would be sufficient to induce the loss of anthracene with concomitant nickel oxidation to generate the $Ni^{IV}\equiv N$ subunit. Instead, dechelation of a phosphine arm occurs. Complex **6.3** is stable at room temperature in solution for several days, and its thermolysis in benzene solution (50-70 °C) produces a new diamagnetic species whose ^1H NMR spectrum definitively shows the presence of the intact dbabh ligand as evident from its signature bridgehead proton resonance near 5.4 ppm. We suspect that the product of this thermolysis reaction is a bridged-amide species, but we have not yet fully characterized this product.

By analogy to the previously reported reactions of $[BP_3]M^IL$ precursors (where $[BP_3]$ = $[PhBP_3]$ and $[PhBP^{iPr}_3]$, M = Fe or Co, L = PMe_3 or PPh_3) with aryl- and alkylazide (RN_3) substrates to generate $M^{III}\equiv NR$ imides,[15,16] similar reactions were pursued with the low valent nickel precursors described herein. The reaction of **6.4** or **6.6** with two equivalents of an organic azide (typical organic azides used: *p*-tolyl-azide, *tert*-butyl azide, 1-adamantyl azide, tosyl azide, and trimethylsilyl azide) in each case produces a mixture of paramagnetic and diamagnetic species that is ill-defined. The phosphine-capped Ni(I) complex **6.4** reacts relatively quickly at room temperature (hours). In contrast, the Ni(I) isocyanide complex **6.6** reacts much more slowly. In the latter case, starting material is still present even after several days at room temperature. Attempts to accelerate the rate of these reactions by heating reaction mixtures of **6.6** in

the presence of azide substrates did lead to more rapid consumption of the nickel precursors, but also to a greater range of spectroscopically detectable species.

We also surveyed the reaction between the Ni^{I}-L precursors and diazoalkanes as potential two-electron carbene transfer reagents. For example, we studied the reactivity of **6.4** and **6.6** in the presence of two equivalents of Ph_2CN_2, Mes_2CN_2, ethyl diazoacetate, and trimethylsilyldiazomethane in benzene solution. Similar to the observations noted above, **6.4** is consumed more rapidly (hours) than **6.6** (days) at ambient temperature for each substrate except Mes_2CN_2, which does not react with either **6.4** or **6.6** over a period of several days at room temperature. The resulting product mixtures invariably contain a variety of unidentified diamagnetic species. The absence of new paramagnetic species in the product profile suggests that a terminal Ni^{III}=CR_2 species is not present.

Finally, we note that the reactivity of the *in situ*-generated Ni(0) species $\{[PhBP^{iPr}_3]NiL\}^-$ **6.7** and **6.8** to group transfer reagents was also examined. These species were generated by reduction of their Ni(I) precursors using sodium amalgam. Quantitative consumption of the Ni(I) species is confirmed by ^{1}H NMR spectroscopy, and subsequent addition of two equivalents of an organic azide or diazoalkane leads in each case to rapid reformation (< 1 h) of the Ni(I) precursor (either **6.4** or **6.6**) in high yield. We suspect that the highly reducing anionic Ni(0) species are acting as electron-transfer reagents and are affecting radical reduction of the organic substrate.

6.2.7. Theoretical considerations

As part of this study, we also undertook the theoretical analysis of several hypothetical nickel complexes featuring a multiply bonded ligand. To contextualize these results, it is useful to consider the work of Hillhouse and coworkers that has provided

isolable Ni=E complexes. Bonding considerations for these complexes have been addressed previously.[34]

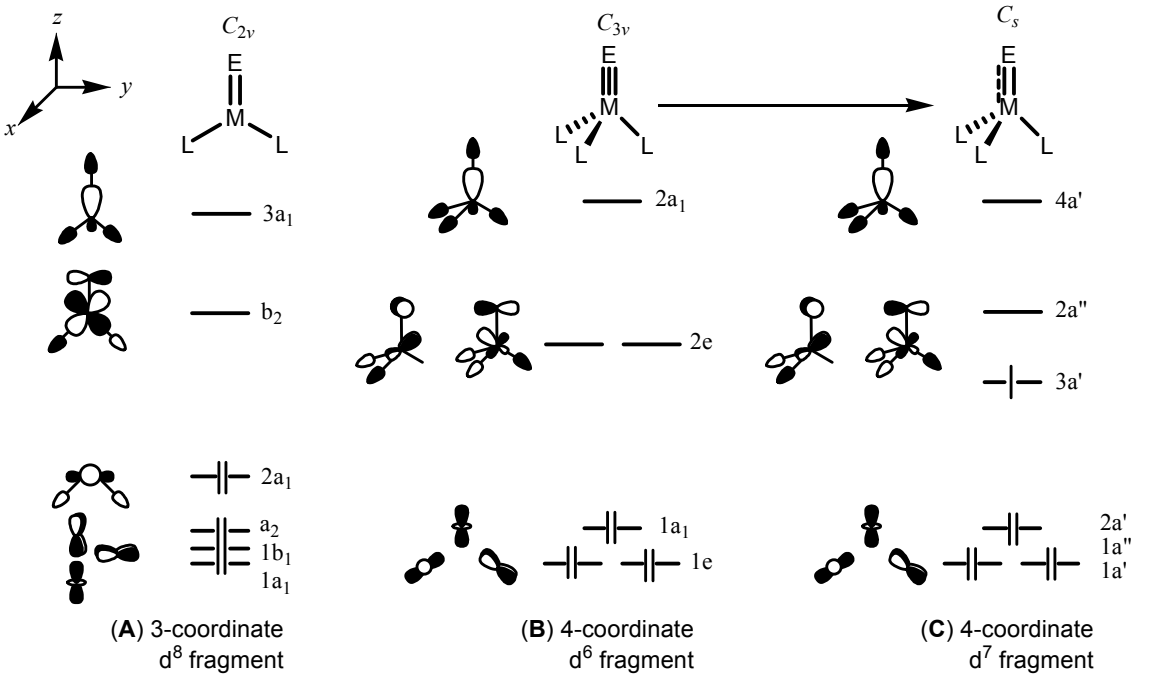

Figure 6.6. Qualitative molecular orbital diagrams for trigonal planar and pseudo-tetrahedral complexes containing Ni=E multiple bonds. Idealized point groups and coordinate axes are indicated.

Figure 6.6A shows lobal representations of the frontier orbitals of an $L_2M{=}E$ fragment as derived from the text by Albright, Burdett, and Whangbo.[35] The LUMO orbital is of b_2 symmetry (under C_{2v}) and is π* in character. The much lower-lying, filled M=E π-bonding orbital is not shown. As a transition is made from the $L_2M{=}E$ fragment to a pseudo-tetrahedral structure under idealized threefold symmetry, the M-E bond is best described as a triple bond (M≡E) for a d^6 configuration (Figure 6.6B).[15,34,36] For a similar geometry with a higher d-count (d^7 or d^8), the formal bond order is lowered as the e-set (under C_{3v}), is π* in character, becomes populated. The d^7 configuration might therefore be expected to be stable for a weakly π-donating fourth ligand. The

[$PhBP_3$]CoI complex provides an example of a species that is d^7 and has a low-spin ground state configuration.[15,37] An interesting issue to consider is the extent to which ligands that are conventionally thought to be more strongly π-donating, such as an imide, will destabilize $L_3M{=}E$ with the d^7 (or d^8) configuration.

We have sought to synthetically prepare complexes that can be formally described as d^6 $L_3Ni^{IV}{\equiv}E$ or d^7 $L_3Ni^{III}{=}E$. Figure 6.6B and C provide the qualitative MO diagrams we expect for such configurations. To examine these structure types theoretically, we have calculated (DFT) hypothetical structures for a series of [$PhBP_3$] and [$PhBP^{iPr}_3$] nickel complexes. As a theoretical control experiment, we performed geometry optimizations for the synthetically isolable and structurally characterized complexes [$PhBP_3$]Ni(NO) and [$PhBP^{iPr}_3$]Ni(PMe_3) (**6.4**). Using the Jaguar computational package (B3LYP/LACVP**), geometry optimizations were performed starting from the crystallographically determined coordinates of [$PhBP_3$]Ni(NO) and **6.4** as the initial starting point. As shown in Figure 6.7 and Table 6.1, the geometry optimized structures for [$PhBP_3$]Ni(NO) and **6.4** compare favorably with those obtained experimentally. One structural distinction worthy of note is that the Ni-P bond distances are approximately 0.1 Å longer in the DFT structures than the experimental structures. Overall, we feel reasonably confident that the theoretical methods used can be expected to give reliable geometries for singlet and doublet configurations in these nickel systems.

Table 6.1. Experimental and calculated bond lengths for **6.4** and [$PhBP_3$]Ni(NO).

6.4	Experimental (Å)	calculated (Å)	[PhBP3]Ni(NO)	Experimental (Å)	calculated (Å)
Ni-P4	2.263	2.358	Ni-N	1.624	1.665
Ni-P1	2.276	2.396	Ni-P1	2.232	2.309
Ni-P2	2.287	2.379	Ni-P2	2.215	2.316
Ni-P3	2.253	2.384	Ni-P3	2.234	2.315
6.4	Experimental (º)	calculated (º)	[$PhBP_3$]Ni(NO)	Experimental (º)	calculated (º)
P4-Ni-P1	121.90	122.45	N-Ni-P1	124.68	123.43
P4-Ni-P2	123.43	124.66	N-Ni-P2	119.84	125.67
P4-Ni-P3	118.67	117.44	N-Ni-P3	124.01	122.58
P1-Ni-P2	98.24	97.50	P1-Ni-P2	92.54	91.54
P1-Ni-P3	92.76	92.17	P1-Ni-P3	95.42	92.93
P2-Ni-P3	94.74	95.12	P2-Ni-P3	91.74	91.29
			Ni-N-O	176.0	177.9

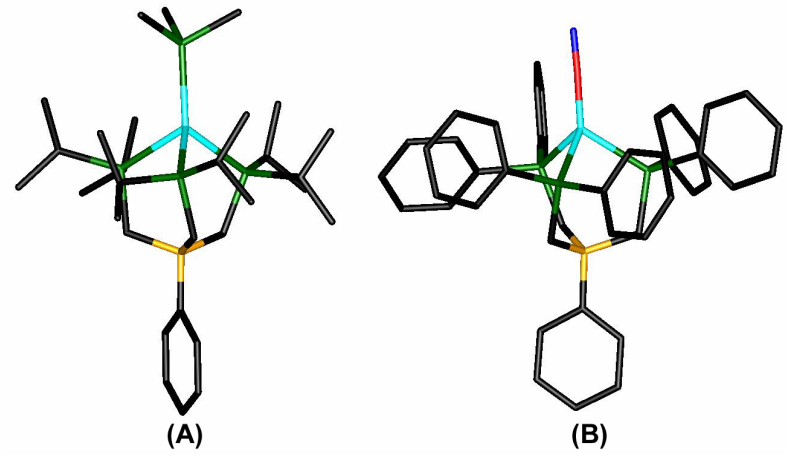

Figure 6.7. DFT optimized (Jaguar 5.0: B3LYP/LACVP**) molecular structures for (A) [$PhBP^{iPr}_3$]Ni(PMe_3) (optimized as a doublet ground state) and (B) [$PhBP_3$]Ni(NO) (optimized as a singlet ground state). Hydrogen atoms have been omitted for clarity.

We next examined the theoretical structures of several hypothetical Ni^{III} imides (Jaguar 5.0: B3LYP/LACVP**). As a starting geometry for the theoretical optimization of S = ½ [$PhBP_3$]Ni(N^tBu), [$PhBP^{iPr}_3$]Ni(N^tBu), and [$PhBP^{iPr}_3$]Ni(NMe), we employed X-ray coordinates for the L_3Ni-N framework analogous to those determined experimentally for S = 0 [$PhBP^{iPr}_3$]Co≡NR and [$PhBP_3$]Co≡NR structures.[15,17] The

theoretical structure for [PhBP$_3$]Ni(N^{t}Bu) is shown in Figure 6.8A. The complex exhibits a short Ni-N bond distance (1.690 Å) that is modestly longer than those observed for [PhBP$_3$]Co≡NR and [PhBP$_3$]Fe≡NR imide structures (1.63-1.67 Å).[15-17] This difference likely reflects the attenuated Ni-N bond order in [PhBP$_3$]Ni(N^{t}Bu). Also of note from the structures is the significant variation in the Ni-P bond distances. One Ni-P distance is significantly longer than the other two (2.429 Å vs. 2.277 and 2.343 Å). The Ni-N-C imide angle is linear (179.28°). A very similar geometry is obtained for the optimized structure of [PhBP$^{iPr}_3$]Ni(N^{t}Bu) (Figure 6.8B). In this latter structure, however, the elongated Ni-P bond distance is considerably further from the nickel center (2.519 Å). Elongation of one of the Ni-P bonds in [PhBP$^{iPr}_3$]Ni(N^{t}Bu) and [PhBP$_3$]Ni(N^{t}Bu) is fully consistent with the presence of a single electron in an orbital that is σ* with respect to a Ni-P bond vector, as illustrated in Figure 6.6C. The distorted geometries we have observed for d^7 [PhBP$_3$]CoX structures provide experimental support for this type of elongation.

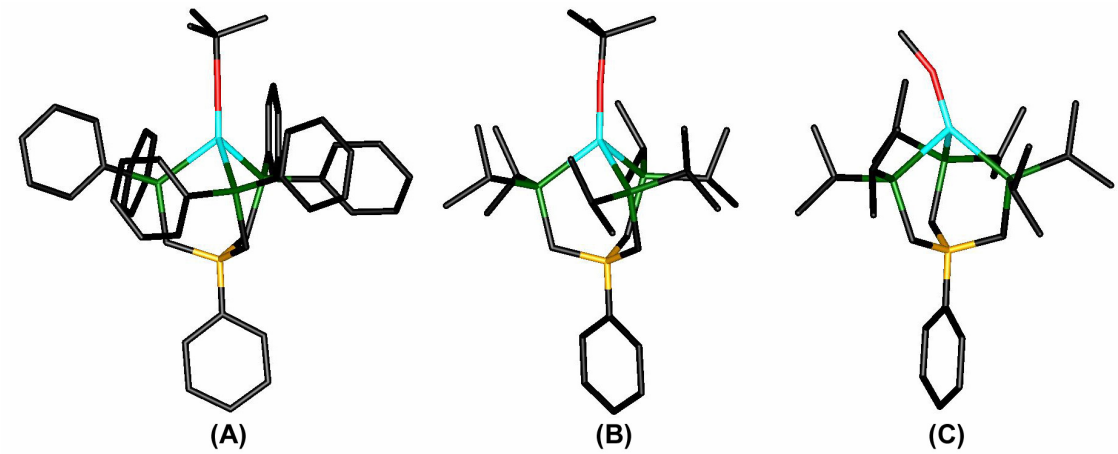

Figure 6.8. DFT optimized (Jaguar 5.0: B3LYP/LACVP**) molecular structures for (A) [PhBP$_3$]Ni(N^{t}Bu), (B) [PhBP$^{iPr}_3$]Ni(N^{t}Bu), and (C) [PhBP$^{iPr}_3$]Ni(NMe). Each geometry assumes a doublet ground state. Hydrogen atoms have been omitted for clarity.

Table 6.2. Bond lengths and angles of DFT optimized structures for $[PhBP_3]Ni(N^tBu)$, $[PhBP^{iPr}_3]Ni(N^tBu)$, and $([PhBP^{iPr}_3]Ni(NMe)$.

	$[PhBP_3]Ni(N^tBu)$	$[PhBP^{iPr}_3]Ni(N^tBu)$	$[PhBP^{iPr}_3]Ni(NMe)$
	Calculated (Å)	Calculated (Å)	Calculated (Å)
Ni-N	1.690	1.687	1.692
Ni-P1	2.429	2.519	2.378
Ni-P2	2.343	2.301	2.368
Ni-P3	2.277	2.303	2.320
	Calculated (º)	Calculated (º)	Calculated (º)
Ni-N-C	179.28	176.90	156.99
P1-Ni-P2	89.85	90.70	94.93
P2-Ni-P3	88.81	92.25	91.90
P1-Ni-P3	89.45	90.78	91.26
N-Ni-P1	122.33	119.83	111.46
N-Ni-P2	126.35	124.54	114.04
N-Ni-P3	128.38	128.40	142.75

To probe whether steric factors might be significantly contributing to the structure observed, the methyl imido complex $[PhBP^{iPr}_3]Ni^{III}(NMe)$ was examined. As can be seen in Figure 6.8C, replacement of the tert-butyl group in $[PhBP^{iPr}_3]Ni(N^tBu)$ for a methyl group in $[PhBP^{iPr}_3]Ni(NMe)$ results in a distortion of the imido ligand such that the Ni-N-C angle is quite bent (156.99°). Moreover, in this latter structure the three Ni-P bond distances show much less variation. Thus, stabilization of the d^7 imide configuration is observed to occur by one of two processes. For a sterically encumbering imide, elongation of one Ni-P bond vector is favored. For an imide that is less bulky, a severe bend in the imide functionality occurs such that a new geometry, better described as trigonal monopyramidal with the imide ligand occupying an equatorial position, is obtained. Collectively, these nickel imide calculations still provide some hope that $L_3Ni{=}NR$ are viable synthetic targets, but synthetic access to them remains to be established.

The final structure of interest concerns the hypothetical nickel nitride $[PhBP^{iPr}_3]Ni^{IV}{\equiv}N$. We are interested in nitrides (or isolobal carbynes) because such functionalities might help to stabilize the unusual Ni(IV) oxidation state. The starting point structure for $[PhBP^{iPr}_3]Ni(N)$ was the same as those used for the nickel imides above except for removal of the alkyl substituent on the imide N-atom, and the calculation assumed a singlet ground state. The starting and final geometries for $[PhBP^{iPr}_3]Ni(N)$ are shown in Figure 6.9A and B, respectively. As can be seen, the nitride group has inserted into one of the Ni-P bonds in the optimized structure. The optimized complex is therefore better viewed as diamagnetic Ni(II) with one phosphinimato and two phosphine ligands. Whether this product is kinetically (or thermodynamically) reasonable is difficult to assess. Bimolecular pathways to other structures, such as a diamond core bridged nitride $Ni^{IV}_2N_2$ or a linear dinitrogen bridged Ni^{I}-N_2-Ni^{I} species, might dominate in solution.

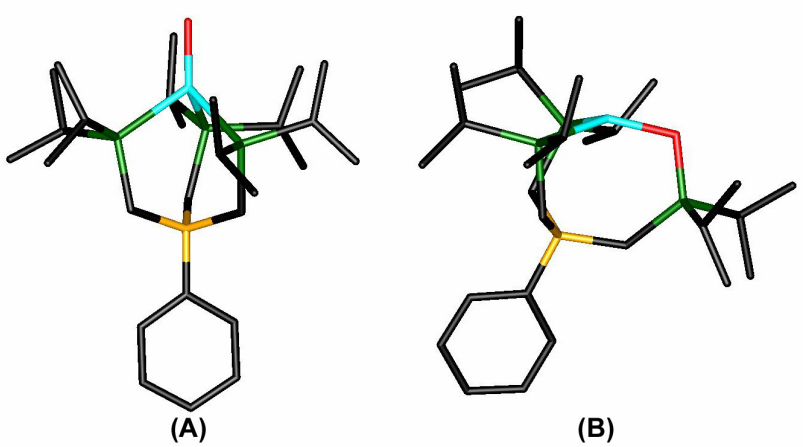

Figure 6.9. Starting point (A) and DFT optimized (Jaguar 5.0: B3LYP/LACVP**) geometry (B) for $S = 0$ $[PhBP^{iPr}_3]Ni(N)$. Hydrogen atoms have been omitted for clarity.

6.3. Conclusions

This chapter discusses the chemistry of the "[PhBP$^{iPr}_3$]Ni" fragment. Most of the complexes described herein, for which the formal oxidation states Ni(0), Ni(I), and Ni(II) have been assigned, give rise to pseudo-tetrahedral geometries. The [PhBP$^{iPr}_3$]-containing Ni(II) complex [κ^2-PhBP$^{iPr}_3$]Ni(dbabh) (**6.3**) is different in that one of the phosphine arms dissociates to provide a three-coordinate trigonal planar structure. A general characteristic of the Ni(II) systems is that access to pseudo-tetrahedral $L_3Ni^{II}X$ complexes where X represents a strong-field alkyl or amide is problematic. This characteristic is also true of Riordan's tris(thioether)borate system [PhTt^{tBu}]Ni^{II}X. Electrochemical studies of the Ni(II) and Ni(I) complexes described reveals that reversible one-electron $Ni^{II/I}$ and $Ni^{I/0}$ redox couples appear to be accessible at low potentials. The $Ni^{III/II}$ redox process is irreversible in all cases that we have examined. We had hoped access to the trivalent nickel state might be possible by turning to dianionic imide and carbene functionalities in the fourth site (L_3Ni^{III}=NR or L_3Ni^{III}=CR_2); however, the successful synthesis of such species has thus far eluded us. Molecular orbital considerations and DFT calculations on hypothetical [PhBP$^{iPr}_3$]Ni=NR and [PhBP$_3$]Ni=NR structures suggest these types of complexes may still be reasonable synthetic targets. We suspect our inability to isolate well-defined examples of these types of species is due to synthetic nuances that we have yet to fully appreciate.

6.4. Experimental section

6.4.1. General considerations

Unless otherwise noted, general procedures were performed according to Section 2.4.1. UV-Vis spectroscopic measurements were recorded on a Varian Cary 50 Bio Spectrophotometer controlled by Cary WinUV Software. All measurements were

recorded using a quartz cell fitted with a Teflon cap. Cyclic voltammetry measurements were recorded using a BAS CV 100W (Bioanalytical Systems Inc., West Lafayette, IN) using a glassy carbon working electrode, a platinum wire auxiliary-electrode and an $Ag/AgNO_3$ non-aqueous reference electrode filled with THF and $[^nBu_4N][PF_6]$. All electrochemical measurements are referenced to Fc/Fc^+ as an internal standard and can be correct to SCE by adding 0.56 V to the reported potential.[38] Solution magnetic moments were measured at 298 K in C_6D_6 following Evans' method.[39]

6.4.2. Starting materials and reagents

The compounds $[PhBP^{iPr}_3]Tl$,[25b] $^iPr_2PCH_2Li$,[40] ASNBr,[41] KC_8,[42] Li{NH(2,6-diisopropylphenyl)}, and Li(dbabh) were prepared according to literature methods. ^{t}BuNC was distilled under dinitrogen and dried over 3Å molecular sieves prior to use.

6.4.3. Syntheses of compounds

$[PhBP^{iPr}_3]NiCl$ (6.1). In a 50 mL round bottom flask, $(DME)NiCl_2$ (283.2 mg, 1.289 mmol) was suspended in THF (15 mL). While stirring vigorously, a THF solution (20 mL) of $[PhBP^{iPr}_3]Tl$ (882.0 mg, 1.286 mmol) was added dropwise over 10 min. After completion of the addition, the reaction mixture was stirred for 25 min and then filtered over Celite on a sintered glass frit. The solids and Celite were washed with benzene (10 mL). The combined filtrates were concentrated to dryness under reduced pressure. The resultant green-brown material was dissolved in benzene (10 mL) and filtered. Lyophilization of the filtrate provided $[PhBP^{iPr}_3]NiCl$ as yellow-green solids (716.8 mg, 96.8%). Crystals of **6.1** were grown from a concentrated solution in diethyl ether at -30 ºC.

^{1}H NMR (300 MHz, C_6D_6): δ 37.1 (br s), 7.2-7.4 (m), 2.5 (br). Magnetic moment (Evans' method, C_6D_6): μ_{eff} = 2.97 μ_B. UV-Vis (C_6H_6) λ_{max}, nm (ε): 720 (330), 425 (3450), 385 (3340). Anal. Calcd. for $C_{27}H_{53}BClNiP_3$: C, 56.34; H, 9.28. Found: C, 56.29; H, 8.92.

[PhBP$^{iPr}_3$]Ni(η^2-CH$_2$P^{i}Pr$_2$) (6.2). A THF solution (2 mL) of ^{i}Pr$_2$PCH$_2$Li (23.3 mg, 0.169 mmol) was added dropwise to a stirring THF solution (2 mL) of **6.1** (95.9 mg, 0.167 mmol). The color of the reaction changed from pale green to yellow. After 30 min, volatiles were removed under reduced pressure. The solids were extracted with benzene (1 mL) and filtered. Volatiles were removed under reduced pressure, providing yellow **6.2** (103.1 mg, 92.0%). Attempts to obtain satisfactory elemental analysis for this compound have not been successful thus far.

^{1}H NMR (300 MHz, C_6D_6): δ 8.01 (br d, 2H, $^3J_{H-H}$ = 6.6 Hz), 7.49 (t, 2H, $^3J_{H-H}$ = 7.5 Hz), 7.26 (t, 1H, $^3J_{H-H}$ = 7.5 Hz), 1.84 (br m, 6H), 1.13 (m, 36H), 0.75 (m, 12H), -0.28 (s, 2H). ^{13}C{^{1}H} NMR (75.4 MHz, C_6D_6): δ 165.6 (q, $^1J_{B-C}$ = 47 Hz), 132.93, 126.77, 123.39, 26.33 (br), 21.08, 20.85, 20.35 (d, J_{P-C} = 6.4 Hz), 19.87 (d, J_{P-C} = 5.1 Hz), 19.71, 19.51 (d, J_{P-C} = 7.4 Hz), -12.84 (doublet of quartets, $^1J_{P-C}$ = 15.9 Hz, $^2J_{P-C}$ = 5.8 Hz). ^{31}P{^{1}H} NMR (121.4 MHz, C_6D_6): δ 49 (br, 3P), -18.2 (q, 1P, $^1J_{P-P}$ = 41 Hz). ^{11}B{^{1}H} NMR (128.3 MHz, C_6D_6): δ -15.7.

[κ^2-PhBP$^{iPr}_3$]Ni(dbabh) (6.3). A diethyl ether suspension (2 mL) of Hdbabh (11.4 mg, 59.0 μmol) was frozen in a liquid nitrogen-cooled well. To the stirring, thawing suspension was added a hexanes solution of n-butyl lithium (1.6 M, 40 μL, 64 μmol). The reaction mixture was stirred and warmed at room temperature for 30 min. The resulting solution and a diethyl ether solution of **6.1** (33.9 mg, 58.9 μmol) were

frozen in a liquid nitrogen-cooled well. The two solutions were thawed, and the thawing solution of **6.1** was added to the thawing solution of Li(dbabh). The yellow-green reaction mixture was stirred and warmed. As the mixture warmed, a color change to inky green brown occurred. After 45 min of warming, the volatiles were removed under reduced pressure. The dark solids were extracted with petroleum ether (3 mL) filtered. Crystals were obtained from the petroleum ether solution by cooling to -30 ºC for several days. The crystals were analyzed as **6.3** (26.4 mg, 61.3%).

^{1}H NMR (300 MHz, C_6D_6): δ 7.75 (d, 2H, $^{3}J_{H\text{-}H}$ = 7.5 Hz), 7.41 (t, 2H, $^{3}J_{H\text{-}H}$ = 7.5 Hz), 7.21 (t, 1H, $^{3}J_{H\text{-}H}$ = 7.2 Hz), 6.98 (dd, 4H, $J_{H\text{-}H}$ = 1.8, 2.7 Hz), 6.72 (dd, 4H, $J_{H\text{-}H}$ = 1.8, 3.0 Hz), 5.44 (s), 1.57 (septet, 6H, $^{3}J_{H\text{-}H}$ = 7.5 Hz), 1.18 (d, 18H, $^{3}J_{H\text{-}H}$ = 7.3 Hz), 1.1 (br m), 0.82 (d, 18H, $^{3}J_{H\text{-}H}$ = 7.5 Hz). ^{31}P{^{1}H} NMR (121.4 MHz, C_6D_6): δ 58 (br). Anal. Calcd. for $C_{41}H_{63}BNNiP_3$: C, 67.24; H, 8.67; N, 1.91. Found: C, 67.18; H, 8.83; N, 1.48.

[PhBP$^{iPr}_3$]Ni(PMe$_3$) (6.4). In a 20 mL vial, [PhBP$^{iPr}_3$]NiCl (227.7 mg, 395.6 μmol) was dissolved in THF (8 mL). Neat PMe_3 (614 μL, 5.93 mmol) was added to the solution, causing the reaction mixture to become dark red. After 10 min, the homogenous reaction mixture was transferred to a vial containing a stirbar and sodium amalgam (0.378% w/w, 2.4022 g, 395 μmol sodium atoms). The reaction mixture was stirred vigorously for 4 h, during which time the color became yellow-orange. The reaction mixture was filtered over Celite on glass fiber filter paper, and the Celite was washed with benzene (3 x 2 mL). The combined filtrates were concentrated to dryness under reduced pressure, providing analytically pure yellow-orange solid **6.4** (239.4 mg,

98.4%). Crystals of **6.4** were grown from a diethyl ether/petroleum ether mixture at -30 ºC.

^{1}H NMR (300 MHz, C_6D_6): δ 35.3 (br s, 6H), 16.5 (br s, 9H), 11.0 (br s, 6H), 10.1 (br s, 18H), 9.0 (s, 2H), 8.0 (t, 2H, J = 7.2 Hz), 7.7 (t, 1H, J = 7.5 Hz), -0.3 (br s, 18H). Magnetic moment (Evans' method, C_6D_6): μ_{eff} = 1.82 μ_B. UV-Vis (C_6H_6) λ_{max}, nm (ε): 430 (1240). Anal. Calcd. for $C_{30}H_{62}BNiP_4$: C, 58.47; H, 10.14. Found: C, 58.50; H, 10.30.

Alternative synthesis: Solid yellow $(COD)_2Ni$ (49.5 mg, 180 μmol) was dissolved in petroleum ether (3 mL). While stirring, neat PMe_3 (75 μL, 725 μmol) was added. After 1 h, a benzene solution (3 mL) of [PhBP$^{iPr}_3$]Tl (123.5 mg, 180.1 μmol) was added to the pale yellow reaction mixture. Upon addition, the reaction mixture darkened. Over 48 h, gray solids precipitated from solution. Volatiles were removed from the reaction mixture under reduced pressure. The solids were extracted with petroleum ether (10 mL) and filtered. Crystallization of the petroleum ether solution at -30 ºC over 3 days provided yellow crystals of **6.4**. Analysis of the crystals by ^{1}H NMR and ^{31}P{^{1}H} NMR spectroscopy showed the presence of [PhBP$^{iPr}_3$]Ni(PMe_3) and [PhBP$^{iPr}_3$]Tl, in a 95:5 ratio.

^{1}H NMR (300 MHz, C_6D_6): δ 35.3 (br s, 6H), 16.5 (br s, 9H), 11.0 (br s, 6H), 10.1 (br s, 18H), 9.0 (s, 2H), 8.0 (t, 2H, J = 7.2 Hz), 7.7 (t, 1H, J = 7.5 Hz), 7.1-7.3 (m, [PhB($CH_2P^iPr_2)_3$]Tl), 1.90 (br, [PhB($CH_2P^iPr_2)_3$]Tl), 1.21 (br, [PhB($CH_2P^iPr_2)_3$]Tl), 1.07 (m, [PhB($CH_2P^iPr_2)_3$]Tl), -0.3 (br s, 18H). ^{31}P{^{1}H} NMR (121.4 MHz, C_6D_6): δ 45.35 (d, $^1J_{Tl\text{-}P}$ = 5910 Hz).

[PhBP$^{iPr}_3$]Ni(CN^{t}Bu) (6.6). To a benzene solution (3 mL) of **6.4** (91.3 mg, 148 μmol) was added dropwise a benzene solution (2 mL) of CN^{t}Bu (67.7 mg, 814 μmol). The reaction mixture darkened to orange-red. The reaction mixture was stirred for 20 min. The solution was filtered and concentrated to dryness under reduced pressure. The resulting orange-red material was dissolved in toluene (1 mL), and concentrated to dryness under reduced pressure. The toluene evaporation procedure was repeated twice more, providing yellow-orange solid **6.6** (78.7 mg, 85.4%). Crystals of **6.6** were grown from a diethyl ether/petroleum ether solution at -30 ºC.

^{1}H NMR (300 MHz, C_6D_6): δ 47.9 (br s, 6H), 12.6 (br s, 6H), 11.3 (br s, 18H), 8.8 (s, 2H), 7.8 (s, 2H), 7.6 (t, 1H, J = 7.5 Hz), 3.0 (s, 9H), 0.3 (br s, 18H). Magnetic moment (Evans method, C_6D_6): μ_{eff} = 1.68 μ_B. UV-Vis (C_6H_6) λ_{max}, nm (ε): 430 (1560). IR (THF, KBr) ν_{CN}: 2056 cm^{-1}. Anal. Calcd. for $C_{32}H_{62}BNNiP_3$: C, 61.67; H, 10.03; N, 2.25. Found: C, 61.39; H, 10.35; N, 2.00.

Alternative synthesis: Solid green **6.1** (81.0 mg, 141 μmol) was dissolved in THF (3 mL). Neat CN^{t}Bu (40 μL, 660 μmol) was added and the reaction mixture was stirred, forming a golden orange solution. After 20 min, the ^{31}P{^{1}H} NMR spectrum was examined. The spectrum was consistent with the formation of square planar [κ^2-PhBP$^{iPr}_3$]Ni(Cl)(CN^{t}Bu) (**6.5**). ^{31}P{^{1}H} NMR (121.4 MHz, THF): δ 62.7 (br d), 47.7 (br d), 3.2 (br s). Volatiles were removed under reduced pressure. The resultant solids were dissolved in THF (2 mL) and added to a sodium amalgam (0.378% w/w, 859.0 mg, 141.2 μmol sodium atoms), washing with additional THF (3 mL). The reaction mixture was stirred vigorously for 3 h. The reaction mixture was filtered, providing an orange-yellow solution. Volatiles were removed under reduced pressure. The resultant solids

were washed with petroleum ether (3 x 0.5 mL), removing an orange-red supernatant and leaving yellow solids. The solids were dried under reduced pressure, providing **6.6** (51.3 mg, 58.4%).

[[κ^2-PhBP$^{iPr}_3$]Ni(CO)$_2$][ASN] (6.9). Solid [PhBP$^{iPr}_3$]Tl (317.1 mg, 0.4625 mmol), $(Ph_3P)_2Ni(CO)_2$ (296.2 mg, 0.4633 mmol), and ASNBr (96.1 mg, 0.466 mmol) were combined in THF (7 mL) and stirred in the dark. Monitoring of the reaction mixture by $^{31}P\{^1H\}$ NMR spectroscopy showed that all of the [PhBP$^{iPr}_3$]Tl had been consumed after 4 d. Volatiles were removed under reduced pressure, and benzene (1 mL) was added to the resulting sticky solids. A yellow oil separated, and the benzene was decanted. This procedure was repeated three times, isolating the yellow oil each time. The yellow oil was placed under reduced pressure for several hours, providing sticky yellow solids. The solids were taken up in a mixture of THF and diethyl ether (2:1), and stored at -30 ºC for 24 hours. A small amount of white precipitate formed, which was removed by filtration. This precipitation process was repeated again. The resulting solution was concentrated to dryness under reduced pressure, to provide sticky yellow solids whose spectroscopic properties were consistent with **6.9** (129.3 mg, 38.7%).

^1H NMR (300 MHz, THF-d_8): δ 7.44 (br s, 2H), 6.87 (t, 2H, J = 7.5 Hz), 6.67 (t, 1H, J = 7.5 Hz), 3.49 (m, 8H), 2.19 (m, 8H), 1.91 (septet, 2H, J = 7.2 Hz), 1.64 (m, 4H), 1.18 (dd, 12H, J = 6.5, 7.2 Hz), 1.08 (m, 4H), 0.97 (m, 12H), 0.77 (dd, 12H, J = 6.2, 7.5 Hz), 0.28 (br, 2H). $^{13}C\{^1H\}$ NMR (75.4 MHz, THF-d_8): δ 208.16 (t, $^2J_{P\text{-}C}$ = 1.6 Hz), 169.08 (q, $^1J_{B\text{-}C}$ = 50 Hz), 133.66, 126.11, 122.20, 63.86 (t, $^1J_{N\text{-}C}$ = 3.2 Hz), 28.23, 27.30, 24.92 (d), 23.03, 21.23 (d), 20.71 (d), 20.45 (d), 20.10 (br), 19.81 (br), 19.73 (d).

$^{31}P\{^{1}H\}$ NMR (121.4 MHz, THF-d_8): δ 51.13 (s, 2P), 4.80 (s, 1P). $^{11}B\{^{1}H\}$ NMR (128.3 MHz, THF-d_8): δ -15.0. IR (THF, KBr) ν_{CO}: 2004, 1878 cm^{-1}.

6.4.4. Computational methods

All calculations were performed using the hybrid DFT functional B3LYP as implemented in the Jaguar 5.0 program package.[43] This DFT functional utilizes the Becke three-parameter functional[44] (B3) combined with the correlation functional of Lee, Yang, and Parr[45] (LYP). The Ni was described using the LACVP basis set with the valence double-ζ contraction of the basis functions, LACVP**. All electrons were used for the other elements using Pople's 6-31G** basis set.[46] Input coordinates were derived as described in the text from crystallographically determined structures. Spin states and molecular charges were explicitly stated, and no molecular symmetry was imposed. Default values for geometry and SCF iteration cutoffs were used, and all structures converged under these criteria.

6.4.5. X-ray experimental information

The general X-ray experimental procedure was performed according to section 2.4.4. Crystallographic information is provided in Table 6.3.

Table 6.3. X-ray diffraction experimental details for **6.1**, **6.3**, **6.4**, and **6.6**.

	6.1	**6.3**
CCDC ID	238112	238115
Chemical formula	$C_{27}H_{53}BClNiP_3$	$C_{41}H_{63}BNNiP_3$
Formula weight	575.57	732.35
T (°C)	-175	-175
λ (Å)	0.71073	0.71703
a (Å)	9.4015(8)	12.0312(10)
b (Å)	11.5998(10)	26.359(2)
c (Å)	29.392(3)	12.9206(11)
α (deg)	90	90
β (deg)	90	99.150(2)
γ (deg)	90	90
V (Å^3)	3205.4(5)	4045.4(6)
Space group	$P2_12_12_1$	$P2_1/n$
Z	4	4
D_{calcd} (g/cm^3)	1.193	1.202
μ (cm^{-1})	8.52	6.27
*R*1, *wR*2 (I > 2σ (I))	0.0392, 0.0717	0.0513, 0.0943

	6.4	**6.6**
CCDC ID	238113	238114
Chemical formula	$(0.95)C_{30}H_{62}BNiP_4$ · $(0.05)C_{27}H_{53}BP_3Tl$	$C_{32}H_{62}BNNiP_3$
Formula weight	(0.95)616.21 · (0.05)685.63	623.26
T (°C)	-175	-175
λ (Å)	0.71703	0.71703
a (Å)	9.6258(5)	9.6300(7)
b (Å)	21.6538(12)	12.2632(9)
c (Å)	16.8244(9)	15.4425(11)
α (deg)	90	87.053(1)
β (deg)	93.871(2)	80.119(1)
γ (deg)	90	84.968(1)
V (Å^3)	3498.8(3)	1788.5(2)
Space group	$P2_1/c$	$P\bar{1}$
Z	4	2
D_{calcd} (g/cm^3)	1.176	1.157
μ (cm^{-1})	9.35	6.97
*R*1, *wR*2 (I > 2σ (I))	0.0534, 0.0925	0.0410, 0.0876

$R1 = \Sigma||F_o| - \Sigma||F_c||/\Sigma|F_o|$, $wR2 = \{\Sigma|w(F_o^2 - F_c^2)^2|/\Sigma|w(F_o^2)^2|\}^{1/2}$

References cited

1) a) Evans, D. A.; Woerpol, K. A.; Hinman, M. M.; Faul, M. M. *J. Am. Chem. Soc.* **1991**, *113*, 726-728. b) Li, Z.; Quan, R. W.; Jacobsen, E. N. *J. Am. Chem. Soc.* **1995**, *117*, 5889-5890. c) Muller, P.; Fruit, C. *Chem. Rev.* **2003**, *103*, 2905-2919. d) Jacobson, E. N. *Comprehensive Asymmetric Catalysis;* Jacobsen, E. N., Pfaltz, A., Yamamoto, H. Eds.; Springer: Hamburg, 1999.

2) a) Doyle, M. P.; McKervey, M. A.; Ye, T. *Modern Catalytic Methods for Organic Synthesis with Diazo Compounds*; Wiley: New York, 1998. b) Brookhart, M.; Studabaker, W. B. *Chem. Rev.* **1987**, *87*, 411-432. c) Doyle, M. P. *Chem. Rev.* **1986**, *86*, 919-939.

3) Collman, J. P.; Hegedus, L. S.; Norton, J. R.; Finke, R. G. *Principles and Applications of Organotransition Metal Chemistry*, 2nd ed.; University Science Books: Mill Valley, CA, 1987.

4) Eisenberg, R.; Fisher, B. *J. Am. Chem. Soc.* **1980**, *102*, 7361-7363.

5) Morgenstern, D. A.; Wittrig, R. E.; Fanwick, P. E.; Kubiak, C. P. *J. Am. Chem. Soc.* **1993**, *115*, 6470-6471.

6) For examples, see: a) Detrich, J. L.; Konečný, R.; Vetter, W. M.; Doren, D.; Rheingold, A. L.; Theopold, K. H. *J. Am. Chem. Soc.* **1996**, *118*, 1703-1712. b) Cecconi, F.; Ghilardi, C. A.; Midollini, S.; Moneti, S.; Orlandini, A.; Bacci, M. *J. Chem. Soc., Chem. Commun.* **1985**, 731-733. c) Ehses, M.; Romerosa, A.; Peruzzi, M. *Top. Curr. Chem.* **2002**, *220*, 107-140. d) Matsunaga, P. T.; Hillhouse, G. L.; Rheingold, A. L. *J. Am. Chem. Soc.* **1993**, *115*, 2075-2077. e) Qin, Z.; Thomas, C. M.; Lee, S.; Coates, G. W. *Angew. Chem., Int. Ed.* **2003**, *42*, 5484-5487. f) Fox, D.

J.; Bergman, R. G. *J. Am. Chem. Soc.* **2003**, *125*, 8984-8985. g) Holland, P. L.; Andersen, R. A.; Bergman, R. G. *J. Am. Chem. Soc.* **1996**, *118*, 1092-1104.

7) *Bioinorganic Catalysis;* Reedijk, J., Bouwman, E. Eds.; Marcel Dekker: New York, 1999.

8) Mindiola, D. J.; Hillhouse, G. L. *J. Am. Chem. Soc.* **2001**, *123*, 4623-4624.

9) Melenkivitz, R.; Mindiola, D. J.; Hillhouse, G. L. *J. Am. Chem. Soc.* **2002**, *124*, 3846-3847.

10) Mindiola, D. J.; Hillhouse, G. L. *J. Am. Chem. Soc.* **2002**, *124*, 9976-9977.

11) Vicic, D. A.; Jones, W. D. *J. Am. Chem. Soc.* **1999**, *121*, 4070-4071.

12) Waterman, R.; Hillhouse, G. L. *J. Am. Chem. Soc.* **2003**, *125*, 13350-13351.

13) Waterman, R.; Hillhouse, G. L. *Organometallics* **2003**, *22*, 5182-8184.

14) Xuliang, D.; Kogut, E.; Wiencko, H. L.; Zhang, L.; Warren, T. H. *Abstracts of Papers,* 224th ACS National Meeting of the American Chemical Society, Boston, MA, Aug 18-22, 2002; American Chemical Society: Washington DC, 2002; INOR 648.

15) Jenkins, D. M.; Betley, T. A.; Peters, J. C. *J. Am. Chem. Soc.* **2002**, *124*, 11238-11239.

16) Brown, S. D.; Betley, T. A.; Peters, J. C. *J. Am. Chem. Soc.* **2003**, *125*, 322-323.

17) Betley, T. A.; Peters, J. C. *J. Am. Chem. Soc.* **2003**, *125*, 10782-10783.

18) Shay, D. T.; Rheingold, A. L.; Zakharov, L. N.; Theopold, K. H. *Abstracts of Papers,* 227th ACS National Meeting of the American Chemical Society, Anaheim, CA, Mar 28 - Apr 1, 2004; American Chemical Society: Washington DC, 2002; INOR 507.

19) Mandimutsira, B. S.; Yamarik, J. L.; Brunold, T. C.; Weiwei, G.; Cramer, S. P.; Riordan, C. G. *J. Am. Chem. Soc.* **2001**, *123*, 9194-9195.

20) Hikichi, S.; Yoshizawa, M.; Sasakura, Y.; Akita, M.; Moro-Oka, Y. *J. Am. Chem. Soc*. **1998**, *120*, 10567-10568.

21) Trofimenko, S. *Scorpionates - The Coordination Chemistry of Polypyrazolylborate Ligands;* Imperial College Press: London, 1999.

22) For examples of Ni complexes supported by [Tp] ligands see: a) Enrique, G.; Hudson, S. A.; Monge, A.; Nicasio, M. C.; Paneque, M. *J. Organomet. Chem.* **1998**, *551*, 215-227. b) Shirasawa, N.; Nguyet, T. T.; Hikichi, S.; Moro-oka, Y.; Akita, M. *Organometallics* **2001**, *20*, 3582-3598. c) Uehara, K.; Hikichi, S.; Akita, M.; Muneta, A. *J. Chem. Soc., Dalton Trans.* **2002**, 3529-3538.

23) Dapporto, P.; Fallani, G.; Sacconi, L. *Inorg. Chem.* **1974**, *13*, 2847-2849.

24) a) Hou, H.; Gantzel, P. K.; Kubiak, C. P. *Organometallics* **2003**, *22,* 2817-2819. b) Hou, H.; Gantzel, P. K.; Kubiak, C. P. *J. Am. Chem. Soc.* **2003**, *125*, 9564-9565.

25) a) Jenkins, D. M.; Di Billo, A. J.; Allen, M. J.; Betley, T. A.; Peters, J. C. *J. Am. Chem. Soc.* **2002,** *124,* 15336-15350. b) Betley, T. A.; Peters, J. C. *Inorg. Chem.* **2003**, *42*, 5074-5084.

26) Zanello, P.; Cinquantini, A.; Ghilardi, C. A.; Midollini, S.; Moneti, S.; Orlandini, A.; Bencini, A. *J. Chem. Soc., Dalton Trans.* **1990**, 3761-3766.

27) The authors report potentials versus SCE and have included the value for Fc/Fc^+ for reference purposes. We state the values corrected relative to Fc/Fc^+ for comparative purposes.

28) Schebler, P.J.; Riordan, C. G.; Guzei, I. A.; Rheingold, A. L. *Inorg. Chem.* **1998**, *37*, 4754-4755.

29) Schebler, P. J.; Mandimutsira, B. S.; Riordan, C. G.; Liable-Sands, L. M.; Incarvito, C. D.; Rheingold, A. L. *J. Am. Chem. Soc.* **2001**, *123*, 331-332.

30) Holland, P. L.; Cundari, T. R.; Perez, L. L.; Eckert, N. A.; Lachicotte, R. J. *J. Am. Chem. Soc.* **2002**, *124*, 14416-14424.

31) Mindiola, D. J.; Cummins, C. C. *Angew. Chem., Int. Ed*. **1998**, *37*, 945-947.

32) Macbeth, C. E.; Thomas, J. C.; Betley, T. A.; Peters, J. C. *Inorg. Chem.* **2004**, *in press*.

33) Betley, T. A.; Peters, J. C. *J. Am.Chem. Soc.* **2004**, *in press*.

34) a) Albright, T. A.; Hoffmann, R.; Tse, Y.; D'Ottavio, T. *J. Am. Chem. Soc.* **1979**, *101*, 3812-3821. b) Albright, T. A.; Hoffmann, R.; Thibeault, J. C.; Thorn, D. L. *J. Am. Chem. Soc.* **1979**, *101*, 3801-3812. c) Glueck, D. S.; Wu, J.; Hollander, F. J.; Bergman, R. G. *J. Am. Chem. Soc.* **1991**, *113*, 2041-2054. d) Cundari, T. R. *J. Am. Chem. Soc.* **1991**, *114*, 7879-7888.

35) Adapted from: Albright, T. A.; Burdett, J. K.; Whangbo, M.-H. *Orbital Interactions in Chemistry,* Wiley & Sons: New York, 1985: pages 365 and 383.

36) Glueck, D. S.; Green, J. C.; Michelman, R. I.; Wright, I. N. *Organometallics* **1992**, *11*, 4221-4225.

37) Shapiro, I. R.; Jenkins, D. M.; Thomas, J. C.; Day, M. W.; Peters, J. C. *Chem. Commun.* **2001**, 2152-2153.

38) For information regarding correcting redox potenials vs Fc/Fc^{+} in various solvents see: Connelly, N. G; Geiger, W. E. *Chem. Rev.* **1996,** *96,* 877-910.

39) a) Evans, D. F. *J. Chem. Soc.* **1959**, 2003-2005. b) Sur, S. K. *J. Magn. Reson.* **1989**, *82*, 169-173.

40) Thomas, J. C.; Peters, J. C. *Inorg. Chem.* **2003**, *42*, 5055-5073.

41) Blicke, F. F.; Hotelling, E. B. *J. Am. Chem. Soc.* **1954**, *76*, 5099-5103.

42) Schwindt, M.; Lejon, T.; Hegedus, L. *Organometallics,* **1990**, *9*, 2814-2819.

43) Jaguar 5.0, Schrodinger, LLC, Portland, Oregon, 2002.

44) Becke, A. D. *J. Chem. Phys.* **1993**, *98*, 5648-5652.

45) Lee, C.; Yang, W.; Parr, R. G. *Phys. Rev. B* **1988**, *37*, 785-789.

46) (a) Hariharan, P. C.; Pople, J. A. *Chem. Phys. Lett.* **1972**, *16*, 217-219. (b) Francl, M. M.; Pietro, W. J.; Hehre, W. J.; Binkley, J. S.; Gordon, M. S.; DeFrees, D. J.; Pople, J. A. *J. Chem. Phys.* **1982**, *77*, 3654-3665.